Earth and Space Science

RESEARCH ARTICLE
10.1029/2022EA002433

Impacts of Horizontal Resolution of the Lateral Boundary Conditions and Downscaling Method on the Performance of RegCM4.6 in Simulating the Surface Climate Over Central-Eastern China

Xiaoke Xu[1], Anning Huang[1], Qian Huang[2], Yan Zhang[3,4], Yang Wu[1], Chunlei Gu[1], Shuxin Cai[1], and Xueyan Zhu[1]

[1]CMA-NJU Joint Laboratory for Climate Prediction Studies, School of Atmospheric Sciences, Frontiers Science Center for Critical Earth Material Cycling, Nanjing University, Nanjing, China, [2]Collaborative Innovation Center on Forecast and Evaluation of Meteorological Disasters, Key Laboratory for Aerosol-Cloud-Precipitation of China Meteorological Administration, Nanjing University of Information Science &Technology, Nanjing, China, [3]Key Laboratory of Radiometric Calibration and Validation for Environmental Satellites, National Satellite Meteorological Center, China Meteorological Administration (LRCVES/CMA), Beijing, China, [4]FengYun Meteorological Satellite Innovation Center (FY-MSIC), Beijing, China

Key Points:

- Direct downscaling method is more suitable to simulate the surface climate over central eastern China than double-nested approach
- Limited impact of the horizontal resolution of reanalysis data for lateral boundary condition generation on the model performance by adopting direct downscaling

Correspondence to:

A. Huang,
anhuang@nju.edu.cn

Citation:

Xu, X., Huang, A., Huang, Q., Zhang, Y., Wu, Y., Gu, C., et al. (2022). Impacts of horizontal resolution of the lateral boundary conditions and downscaling method on the performance of RegCM4.6 in simulating the surface climate over central-eastern China. *Earth and Space Science*, *9*, e2022EA002433. https://doi.org/10.1029/2022EA002433

Received 19 MAY 2022
Accepted 4 JUL 2022

Author Contributions:

Conceptualization: Anning Huang, Qian Huang
Data curation: Xiaoke Xu, Yan Zhang, Yang Wu, Shuxin Cai, Xueyan Zhu
Formal analysis: Xiaoke Xu
Funding acquisition: Anning Huang
Investigation: Xiaoke Xu, Yan Zhang
Methodology: Xiaoke Xu, Anning Huang
Resources: Xiaoke Xu, Yang Wu, Xueyan Zhu
Supervision: Anning Huang
Validation: Xiaoke Xu, Anning Huang
Visualization: Xiaoke Xu, Chunlei Gu, Shuxin Cai
Writing – original draft: Xiaoke Xu, Anning Huang
Writing – review & editing: Anning Huang, Qian Huang, Chunlei Gu

Abstract This study investigated the impacts of horizontal resolution of lateral boundary condition (LBC) and downscaling method on the performance of RegCM4.6 in simulating the 2 m air temperature and precipitation over central eastern China. Two groups of experiments (direct downscaling experiments using LBC derived from the same reanalysis data but with different horizontal resolutions [0.75°, 1.5°, and 2.5°] and double-nested downscaling experiment) with the model horizontal resolution of 20 km over central eastern China have been carried out. Results show that the direct downscaling experiments consistently outperform the double-nested experiment to simulate the 2 m air temperature and precipitation over central eastern China, suggesting that adopting the direct downscaling method is appropriate to simulate the surface climate over central eastern China. Meanwhile, the direct downscaling experiments driven by the LBC derived from the reanalysis data with the horizontal resolution ranging from 0.75° to 2.5° display very comparable performance with a little better performance by adopting the LBC derived from the reanalysis data of much finer resolution. Further mechanism analysis indicates that much larger errors of LBC produced by the double-nested downscaling method lead to the positive pressure biases and negative biases of water vapor convergence flux over Jianghuai Valley, which contribute to the much larger biases of precipitation and 2 m air temperature in the double-nested downscaling experiment compared to the direct downscaling experiments. This study emphasizes that the direct downscaling method is superior to the double-nested downscaling method for the simulations of 2 m air temperature and precipitation over central eastern China.

1. Introduction

The regional climate models (RCMs) are important tools as they act as a bridge between the global climate models (GCMs) with coarse resolution and small-scale processes that required finer resolution. RCMs with higher resolution and flexible physical parameterizations have proved successful in representing both the basic features of large-scale atmospheric circulations and a wide range of mesoscale phenomena (Chen et al., 2019; Gao & Giorgi, 2017; Giorgi & Mearns, 1999; Park et al., 2013). Several aspects affecting the performance of RCMs are summarized as follows: (a) The dynamical framework, such as the hydrostatic core and nonhydrostatic core (Adeniyi, 2020; Kalmar et al., 2018); (b) the physics parameterizations, including the cumulus convective scheme, lateral boundary scheme, large-scale moisture scheme, and radiation and land surface parameterizations (Gao et al., 2016; Gu et al., 2020; Zhang et al., 2015); (c) the model spatial resolution (even 60 km higher resolutions are necessary to accurately reveal the revolution of climatic precipitation over China and East Asia (Gao et al., 2006; Gao et al., 2017b)); (d) the different nesting techniques such as Big-Brother Experiments (Denis, Côté, & Laprise, 2002, Denis, Laprise, et al., 2002), two-way nesting technique (Combes & Matano, 2014; Qi et al., 2018), and one-way or one-way double-nested strategy (Diallo et al., 2018; Im et al., 2006; Leung & Qian, 2003); (e) the quality of initial conditions (IC) and lateral boundary conditions (LBC) (Laprise et al., 2012;

Leps et al., 2019); and (f) the domain size and location of LB (Maurya et al., 2018; Wu et al., 2005; Xue et al., 2014), etc.

A series of studies have shown that the LBC of RCMs is crucial for long-term simulation (Denis et al., 2003; Giorgi & Mearns, 1999). The data quality and spatial and temporal resolutions of LBC are closely related to the uncertainty in RCM simulations (Amengual et al., 2007; Denis, Laprise, et al., 2002; Giorgi & Mearns, 1999; Seth et al., 2007; Wu et al., 2005). Among the commonly used reanalysis data to provide LBC for RCMs, compared with FNL (NCEP-FNL reanalysis data), EC data (ERA-Interim reanalysis data) tend to be more appropriate to provide IC and LBC in RCMs (Bromwich et al., 2013; Huang & Gao, 2018; Meng et al., 2018). Meanwhile, whether the LBC generated by the same reanalysis data but with much higher resolutions brings the better skill of RCMs or not also has different viewpoints (Amengual et al., 2007; Liu et al., 2011; Marbaix et al., 2003; Meng et al., 2018). Some of them believe that the differences in the simulations of surface climate and summer mean distribution by adopting the LBC derived from the reanalysis with different resolutions are notably larger (Liu et al., 2011; Marbaix et al., 2003). Other researchers think that the model skill is not appreciably improved by increasing the resolution of LBC (Amengual et al., 2007; Meng et al., 2018). In addition, the LBC with a temporal resolution higher than 12 hr can significantly improve the RCM simulations of air temperature and precipitation (Amengual et al., 2007; Denis et al., 2003). Therefore, what is the effect of the LBC horizontal resolution in RCMs and how to choose the appropriate resolution of reanalysis data to provide the IC and LBC for RCMs need to be further analyzed.

Besides the direct downscaling method, Leung and Qian (2003) put forward a strategy of one-way double-nested approach: The RCMs at the grid spacing with a higher resolution are driven by nesting their own simulations with a coarse resolution. Previous studies indicate the performance difference between the double-nested and the direct downscaling method (Cui et al., 2007; Diallo et al., 2018; Hu et al., 2015; Ji & Kang, 2013; Wu et al., 2012). The main conclusions are divided into two points: (a) The double-nested downscaling method can significantly improve the model performance (Diallo et al., 2018; Gao et al., 2006; Im et al., 2006; Ji & Kang, 2013). (b) Double-nested downscaling method shows no improvement or even worse performance relative to the direct downscaling method (Beck et al., 2004; Hu et al., 2015; Nguyen-Xuan et al., 2021; Raffa et al., 2021; Wu et al., 2012). The main reasons for this contrary viewpoint are attributed to the double-nested downscaling method being regional-dependent (Hong et al., 2010; Im et al., 2006) and case-dependent (Gu et al., 2020; Raffa et al., 2021). In complex terrains, such as mountainous and plateau areas, using the double-nested downscaling method can obtain better model performance (Diallo et al., 2018; Gao et al., 2006; Im et al., 2006; Ji & Kang, 2013). However, in the area of flat terrains, such as central and eastern Europe, the double-nested downscaling method does not significantly improve the skills of the model compared with the direct downscaling method (Beck et al., 2004; Pavlik et al., 2012; Raffa et al., 2021).

Central eastern China is the most populous and economically developed region containing a part of the northwest plateau, the southern hills, and the eastern plain; and it is largely affected by the East Asian monsoon (Meng et al., 2018; Nguyen et al., 2021). As the region with frequent meteorological disasters, the climate prediction accuracy over central eastern China is low and controlled by a monsoon climate. However, few studies reveal the impacts of the horizontal resolution of LBC and downscaling method on the performance of RegCM in simulating the surface climate over central eastern China. It is essential to improve the level of refinement prediction of RCMs. This work aims to examine the sensitivity of RegCM version 4.6 (RegCM4.6) performance to the downscaling strategy (direct downscaling method and double-nested downscaling method) and the horizontal resolution of reanalysis used in the direct downscaling method in simulating the surface air temperature and precipitation over central eastern China in summer. For this purpose, we will answer such questions as follows: How do the downscaling methods affect the performance of RegCM4.6 in simulating the near-surface air temperature and precipitation over central eastern China? What kind of horizontal resolution for the LBC of RegCM4.6 is more appropriate over central eastern China? What are the underlying mechanisms related to the differences in the model results? Fully understanding and answering these questions can make it much quicker to choose appropriate LBC for RCMs. It can also help to deepen our comprehension of the nesting technique in the gradually refined RCMs and provide the necessary reference for further improving the simulation and prediction level of RCMs in central eastern China.

2. Model, Data, Experiment, and Method

2.1. Model

The fourth regional climate model from the International Centre for Theoretical Physics (ICTP) RegCM4.6 (https://www.ictp.it/research/esp/models/regcm4.aspx) (Giorgi et al., 2012) is used in this study. It has undergone a series of improvements (Giorgi, Marinucci, & Bates, 1993, Giorgi, Marinucci, Bates, & De Canio, 1993; Giorgi & Mearns, 1999; Pal et al., 2007). RegCM4.6 has added a variety of options, including a nonhydrostatic dynamic framework (Giorgi et al., 2012), radiation transfer scheme (Kiehl et al., 1996), chemical aerosol reaction scheme (Park et al., 2013), cumulus convection parameterization (Emanuel and Zivkovic, 1999), and more sophisticated cloud microphysics parameterization (Nogherotto, 2015; Nogherotto et al., 2016). These make it possible to capture refined climate features at a regional scale. This model has been validated in the East Asian monsoon region with complex topography (Gao et al., 2016, 2017b; Shi et al., 2018). In addition, the RegCM has been widely verified in the applicability assessment (Gao et al., 2016; Gu et al., 2020; Zhang et al., 2015), climate prediction (Gu et al., 2012; Pan et al., 2020; Shi et al., 2018), and mechanism research of extreme climate events (Kong et al., 2019; Ngo et al., 2017) in China.

2.2. Data

To provide the IC and LBC for the RegCM4.6 in this study, we adopted the 6-hourly global reanalysis data with three different horizontal resolutions from the European Centre for Medium-Range Weather Forecasts (ECMWF) (http://apps.ecmwf.int/datasets/data/Interim-full-daily/levtype=sfc/): (a) The ERA40 data, which is the second generation of reanalysis of ECMWF with the horizontal resolution of 2.5° × 2.5° during 1957–2002. It is widely used in various researches (Hassan et al., 2015; Heikkilä et al., 2011; Hu et al., 2010; Wang et al., 2015) and exhibit extensive and accurate descriptions of the atmospheric characteristics (Zhao & Fu, 2006). (b) The EIN15 data with the horizontal resolution of 1.5° × 1.5° from 1979 to the present. (c) The EIN75 data with the horizontal resolution of 0.75° × 0.75° from 1979 to the present (Zhao et al., 2010). Both EIN15 and EIN75 data were expanded from ERA40 via a preferable performance of observing systems and predictability of atmospheric processes (Dee et al., 2011). Additionally, all experiments used the same sea surface boundary, which was provided by the National Oceanic and Atmospheric Administration (NOAA) Optimum Interpolation (OI) SST V2 data with the horizontal of 1° from 1981 to the present (Reynolds et al., 2002). It is available at https://www.psl.noaa.gov/data/gridded/data.noaa.oisst.v2.html.

To validate the outputs of RegCM4.6, we used the data listed as follows: (a) The fifth generation of ECWMF atmospheric reanalysis data (ERA5) with the horizontal resolution of 0.25° and temporal resolution of 24 hr from 1979 to the present (Copernicus Climate Change Service (C3S), 2017), which is available at https://cds.climate.copernicus.eu/cdsapp%23%21/search%3Ftype%3Ddataset. It has good accuracy in the Yangtze River Basin, China (Fu et al., 2021; Zhang et al., 2019). (b) The daily observed precipitation data set SURF_CLI_CHN_PRE_MON_GRID_0.5_V2.0, which is produced by interpolating the gauge-observed precipitation at ∼2,400 stations over China from 1961 to the present with the consideration of GTOPO30 (Global Digital Elevation Model Data) topographic distribution onto the grids with the horizontal resolution of 0.5° (Zhao et al., 2014) (available at the site http://data.cma.cn/).

2.3. Numerical Experimental Design

We designed two groups of experiments shown in Figure 1:

1. **Direct downscaling experiments**: The RegCM4.6 is run at 20 km grid spacing (Figures 1b and 1d) with the IC and LBC derived from the EC reanalysis data with different horizontal resolutions. And we named the experiments Exp2.5, Exp1.5, and Exp0.75 corresponding to the IC and LBC derived from the EC data with the horizontal resolution of 2.5°, 1.5°, and 0.75°, respectively.
2. **Double-nested experiment**: The RegCM4.6 is first run at 50 km grid spacing in the "mother" domain (Figure 1c) driven by the IC and LBC obtained from the EC reanalysis data with the horizontal resolution of 1.5° and then the model is run at 20 km grid spacing in the nested domain, which is the same as the direct downscaling experiments (Figure 1d), with the IC and LBC derived from the 50-km simulations of RegCM4.6 in the "mother" domain. We named this experiment as Nest_Exp.

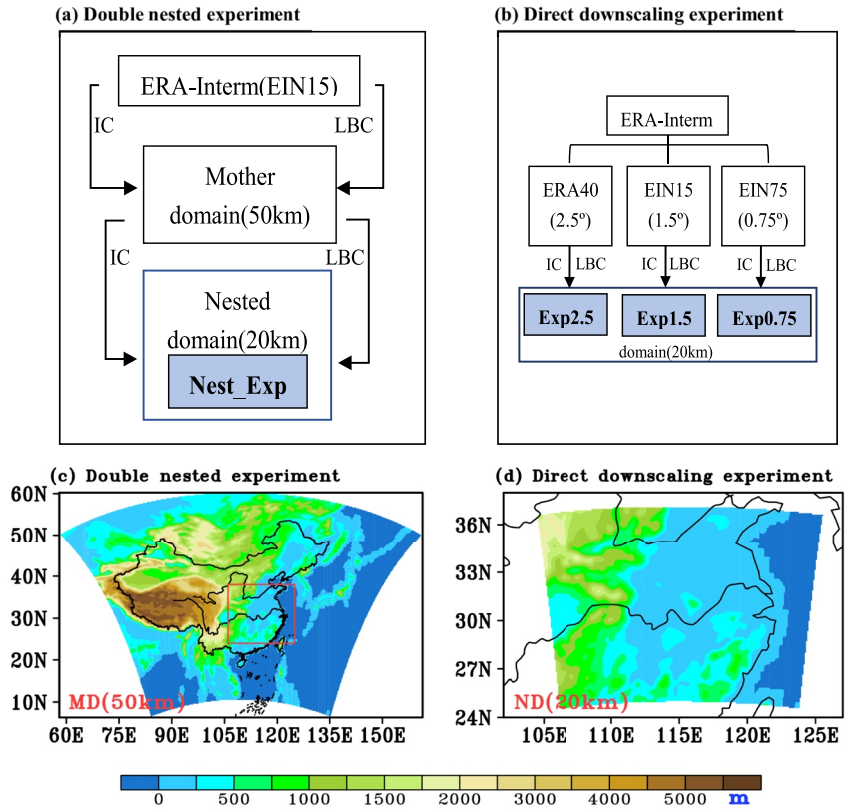

Figure 1. Flowchart of two group experiments (a and b). For the Nest_Exp (a), the initial conditions (IC) and lateral boundary Condition (LBC) of RegCM4.6 in the mother domain are derived from the EIN15 data, while those in the nested domain are derived from the 50 km simulations of RegCM4.6 in the mother domain (c). For the direct downscaling experiments (b), the IC and LBC of RegCM4.6 in the 3 experiments are derived from the ECMWF data of 3 horizontal resolutions with the same domain as the nested domain for the Nest_Exp (d). Shadings in (c) and (d) show the terrain height.

The model domain covers central eastern China and is centered at 31°N, 115°E with the 96 × 72 grids and 12 grids for the lateral boundary buffer zone. The RegCM4.6 adopts 18 vertical layers in the atmosphere and a model time step of 60 s. The model integration starts on 1 January 1988 and ends on 31 December 1999 for each experiment with the first 3 months as spin-up time (Zhong et al., 2007). The physical parameterizations in this study are as follows: The modified CCM3 radiation scheme (Kiehl et al., 1996), the BATS land surface scheme (Dickinson, 1993), the UW-PBL planetary boundary layer scheme (Bretherton et al., 2004)), the MIT cumulus convection scheme (Emanuel and Zivkovic, 1999), the ocean flux scheme (Zeng et al., 1998), and the SUBEX large-scale precipitation scheme (Pal et al., 2000). It is worth noting that the lateral boundary condition scheme used in this study is the relaxation scheme (Marbaix et al., 2003), which makes a relaxation component continuously added to the model-generated fields in an appointed "buffer zone" to decrease the deleterious effects that account for large-scale data of boundary and finer internal field. All data are interpolated to the model resolution (20 km) for analysis using a bilinear interpolation method (Diaconescu et al., 2015; Huan et al., 2018).

2.4. Method

To quantify the model performance, we defined a comprehensive index called Rtr, which is the ratio of Taylor Score (Taylor, 2001) to the normalized root mean square error (NRMSE). The formula for the Rtr score is given by

$$Rtr = \frac{TS}{NRMSE} \quad (1)$$

where TS is the Taylor score, which evaluates both pattern and amplitude of variability. The specific formula is given by

$$TS = \frac{4(1+R)}{\left(\sigma + \frac{1}{\sigma}\right)^2 (1+R_0)} \tag{2}$$

where R is the pattern correlation between observation and simulation, σ is the modeled spatial standard deviation divided by that of observation, and R_0 is an achievable maximum correlation (here, set as 1). Consequently, the TS ranges from 0 to 1. A larger TS indicates better performance in simulating the pattern and amplitude of variability (Kan et al., 2015).

In addition, the NRMSE used in this study is as follows:

$$\mathrm{NRMSE} = \frac{\sqrt{\frac{1}{n}\sum_{i=1}^{n}(S_i - \mathrm{O}_i)^2}}{\frac{1}{n}\sum_{i=1}^{n} O_i} \tag{3}$$

where S_i and O_i are the values of simulation and observation. n is the number of model grids. Smaller $NRMSE$ indicates better performance in simulating quantity. Therefore, larger Rtr represents higher skill.

The pattern correlation coefficient (PCC) is used in this study to evaluate the performance of surface climate in central eastern China. The formula is as follows:

$$\mathrm{PCC} = \frac{\frac{1}{n}\sum_{i=1}^{n}\left(S_i - \overline{S}\right)\left(O_i - \overline{O}\right)}{\sqrt{\frac{1}{n}\sum_{i=1}^{n}\left(S_i - \overline{S}\right)^2}\sqrt{\frac{1}{n}\sum_{i=1}^{n}\left(O_i - \overline{O}\right)^2}} \tag{4}$$

where $\overline{S}$ and $\overline{O}$ are the area average of the nested domain of simulation and observation. Furthermore, the water vapor convergence flux (WVCF) is calculated to evaluate the convergence and ascending motion or the divergence and descending motion over a region based on the moisture budget equation (Hsu et al., 2012; Huang et al., 2014):

$$\mathrm{WVCF} = -\frac{1}{g}\int_{300}^{P_s} \nabla \cdot \left(q\vec{V}\right) \mathrm{d}p \tag{5}$$

where q is specific humidity ($\mathrm{g \cdot g^{-1}}$), $\vec{V}$ is the horizontal wind vector ($\mathrm{m \cdot s^{-1}}$), g is the acceleration of gravity ($\mathrm{m \cdot s^{-2}}$), and P_s is surface air pressure (hPa).

3. Results

3.1. Model Evaluation

Figure 2 shows the spatial distribution of the summer mean 2 m air temperature and precipitation in central eastern China during 1989–1999 from observation and simulation. The observed 2 m air temperature exhibits a high-temperature center (over 28°C) located in the region covering from 110°E to 117°E and 26°N to 30°N (Figure 2a). The experiments of the direct downscaling method can well reproduce the spatial distribution of the observed 2 m temperature with the PC more than 0.8 (Figures 2b–2d) but the double-nested experiment cannot well reproduce the observed high 2 m air temperature centered over the area north to Yangtze River (Figure 2e). From Figure 2f, the observed summer mean precipitation decreases from southeast to northwest with a strong center over 10 mm $\mathrm{d^{-1}}$ located in the area south of Yangtze River. The direct downscaling (Figures 2g–2i) can reproduce the overall spatial distribution of the observed precipitation with the PCC coefficients between the simulation of direct downscaling and observation over 0.4. However, the Nest_Exp produced a PCC of −0.23 (Figure 2j), indicating that the precipitation simulated by the Nest_Exp cannot reproduce the spatial distribution characteristics compared to the observation.

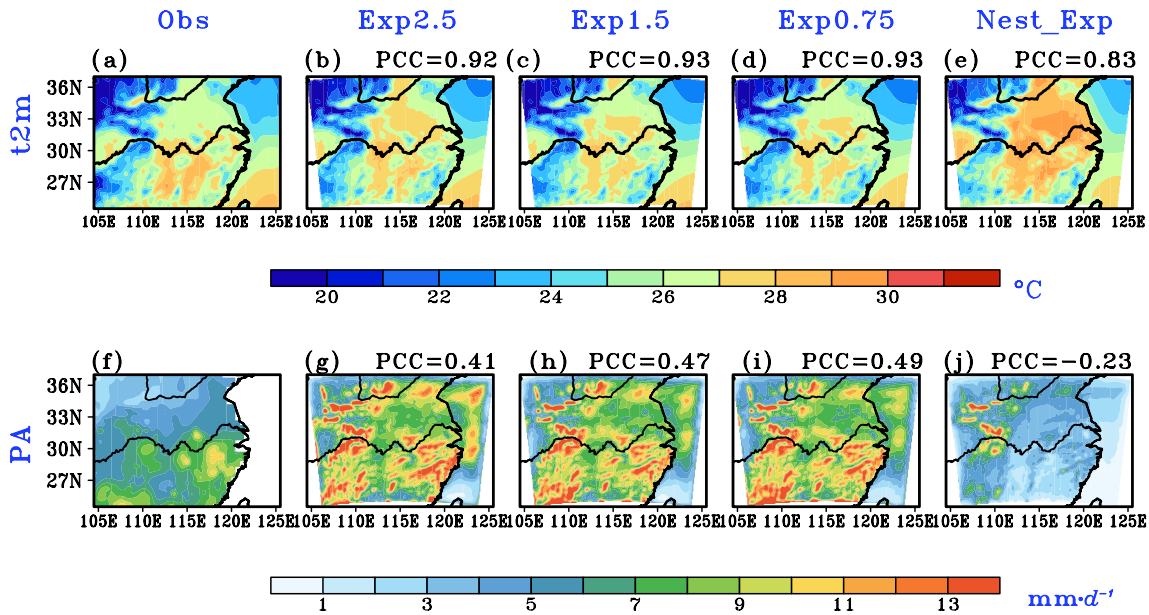

Figure 2. The spatial distribution of observed and simulated summer mean 2 m temperature and precipitation amount averaged during 1989–1999. Pattern correction coefficients between simulation and observation are shown in the top right corner of each subplot.

As a whole, the direct downscaling tends to show relatively higher skill in simulating the spatial pattern of 2 m air temperature and precipitation than the Nest_Exp. Meanwhile, relatively higher skill can be obtained by adopting the reanalysis data with the relatively finer horizontal resolution to generate the LBC of the RegCM4.6 model.

Figure 3 further gives the bias of 2 m air temperature and precipitation produced by each experiment. From Figures 3a–3d, all direct downscaling experiments tend to overestimate (underestimate) the air temperature over Jianghuai Valley (northwest and southeast parts of the model domain) by ∼1°C–2°C (Figures 3a–3c), and the model biases are decreased with the horizontal resolution of the reanalysis data for the LBC increased. The

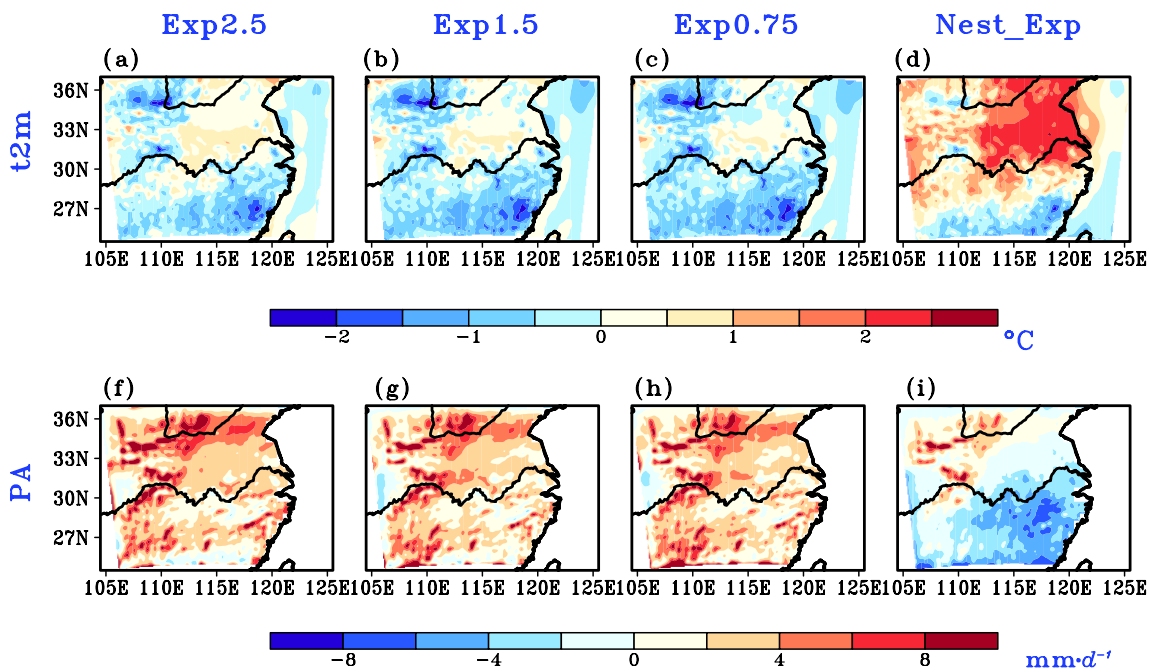

Figure 3. The distribution of biases in the simulated 2 m temperature and precipitation amount to the observation in summer averaged during 1989–1999.

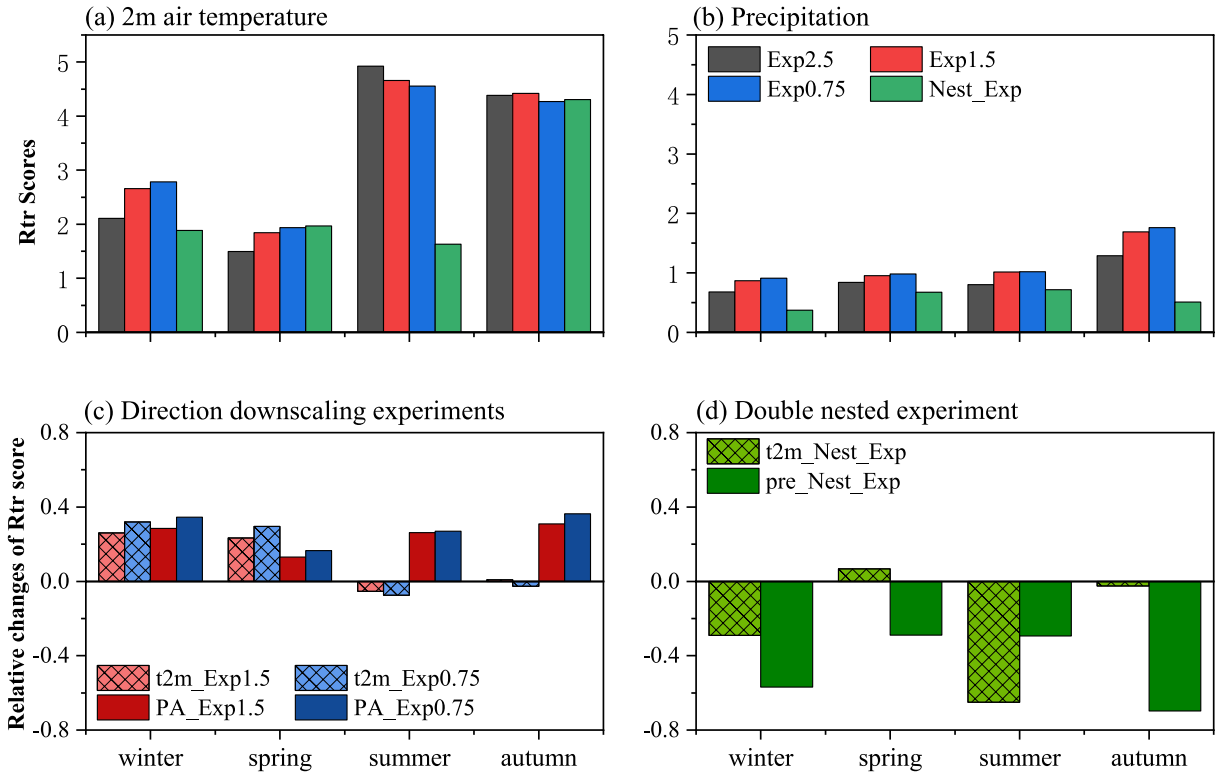

Figure 4. Rtr score of each experiment in simulating the 2 m air temperature (a) and total precipitation (b) in the region bounded by 110–120°N and 27–35°E during 1989–1999. Relative changes of Rtr scores produced by Exp1.5 and Exp0.75 experiments relative to Exp2.5 experiment in simulating 2 m air temperature and precipitation (c) and relative changes of Rtr score produced by the Nest_Exp experiment relative to the Exp1.5 experiment in simulating 2 m air temperature and precipitation (d).

Nest_Exp (Figure 3d) that produced the distribution of biases in the 2 m air temperature is consistent with those simulated by the direct downscaling method. Whereas, the extension and intensity of the warm biases produced by Nest_Exp are much larger and stronger than the results of the direct downscaling experiment. From Figures 3f–3h, all of the direct downscaling experiments overestimated the precipitation over most model domains with a very similar spatial distribution of precipitation biases: Three large bias centers with intensity over 4 mm d^{-1} are located over the north, central west, and southwest parts of the model domain. While the Nest_Exp shows underestimation (overestimation) with the intensity of 4 mm d^{-1} over the southeast (northwest) part of the model domain (Figure 3i).

To comprehensively evaluate each experiment in simulating the spatial pattern and intensity of 2 m air temperature and precipitation, Figure 4 provides the Rtr score of the simulated 2 m air temperature and precipitation in different seasons. From Figure 4a, the Rtr scores for 2 m air temperature simulation show profound seasonal differences with much larger values in summer (June, July, and August) and autumn (September, October, and November) than winter (December, January, and February) and spring (March, April, and May), implying that the RegCM4.6 model shows much better performance to simulate the 2 m air temperature in summer and autumn than in spring and winter. Meanwhile, among the 4 seasons, the Rtr difference between each direct downscaling experiment and Nest_Exp is the highest in summer, suggesting that the simulations of 2 m air temperature in summer with the LBC directly derived from the reanalysis data have much higher skill than those with the LBC generated by the double-nested downscaling method. Moreover, the Nest_Exp shows comparable (slightly better) skill in simulating the 2 m air temperature to the direct downscaling experiments in autumn (spring), while the Nest_Exp displays much worse skill relative to the direct downscaling experiments in winter and summer, indicating that the differences of skill in simulating the 2 m air temperature induced by adopting different downscaling strategies are highly dependent on the season (Hu et al., 2015; Im et al., 2006).

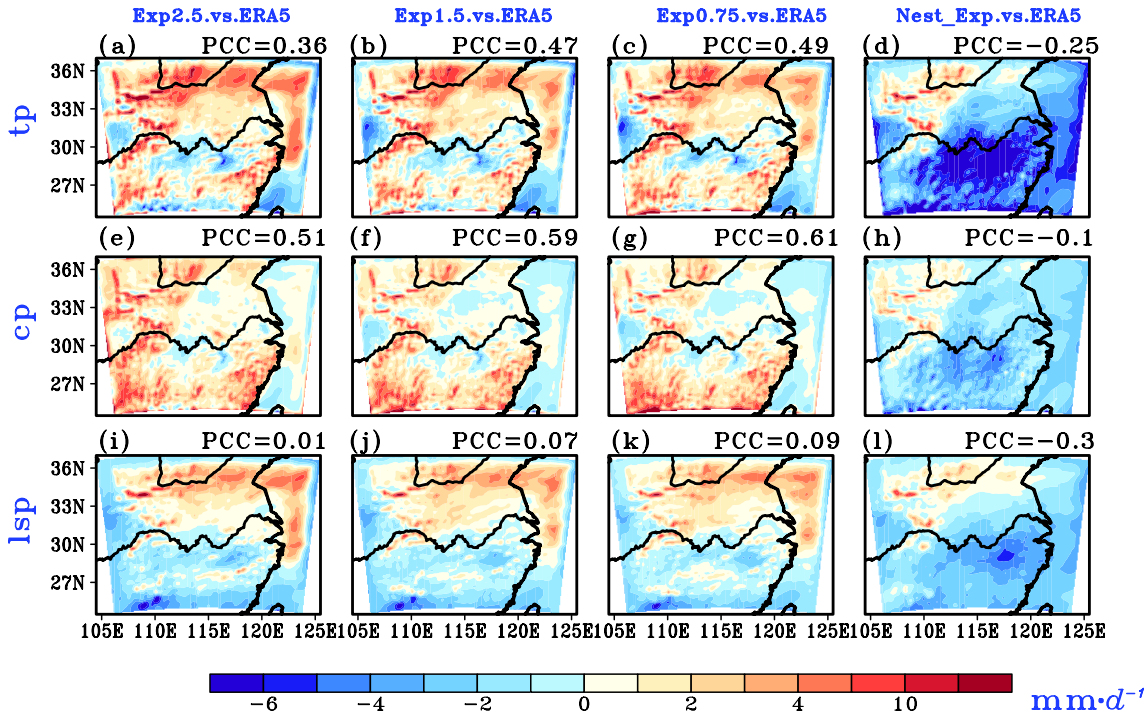

Figure 5. The differences of total (a–d), convective (e–h), and large-scale precipitation (i–l) relative to ERA5 in summer averaged during 1989–1999. The pattern correlation coefficient between simulation and observation is shown in the top right corner of each subplot.

Compared to the situation of 2 m air temperature simulation, precipitation simulation shows relatively lower skill in all seasons (Figure 4b) because precipitation is a complicated variable resulting from atmospheric circulations, which reflects the interaction of energy, mass, and momentum (Chen et al., 2019). Generally, the comprehensive skill of the direct downscaling method is distinctly better than the double-nested downscaling method in all seasons. And the largest Rtr differences between each direct downscaling experiment and Nest_Exp are shown in autumn among the 4 seasons (Figure 4b). From the direct downscaling experiments (Figure 4c), the relative changes of Rtr scores produced by the Exp1.5 and Exp0.75 experiments relative to the Exp2.5 experiment are positive during most seasons in simulating the 2 m air temperature and precipitation except slightly negative changes in summer and autumn for the precipitation simulation, demonstrating that the model skill in simulating the 2 m air temperature and precipitation can be slightly improved by adopting the LBC derived from the reanalysis data with relatively higher horizontal resolutions. Meanwhile, compared to the EXP1.5 experiment with the direct downscaling method, the Nest_Exp produced a much lower Rtr score in simulating 2 m air temperature and precipitation in most seasons (Figure 4d), indicating that better performance can be obtained by adopting the direct downscaling method.

3.2. Possible Mechanism Related to the Difference in the Model Performance

As the rainy season for central eastern China is concentrated in summer, we will take summer as an example to discuss the possible causes related to the skill difference in simulating the precipitation among the four experiments. Figure 5 further gives the distribution of differences in the simulated total precipitation (TP), convective (CP), and large-scale precipitation (LSP) in each experiment relative to ERA5 in summer averaged during 1989–1999. As mentioned above, the ERA5 data have good accuracy in the Yangtze River Basin, China (Fu et al., 2021; Zhang et al., 2019) and provide large-scale and convective precipitation data, which do not exist in gauge observation. From Figures 5a–5d, the differences in TP show very similar features to the gauge observations (not shown), indicating that the ERA5 data can be used to evaluate the model simulation (Chu et al., 2017; Kan et al., 2015). For the CP, the wet biases produced by the direct downscaling experiments are concentrated in the south and northwest parts of the model domain with complex terrain (Figures 5e–5g). It may be related to the fact that the convective process is influenced by the rugged land surface that is more likely to trigger convective

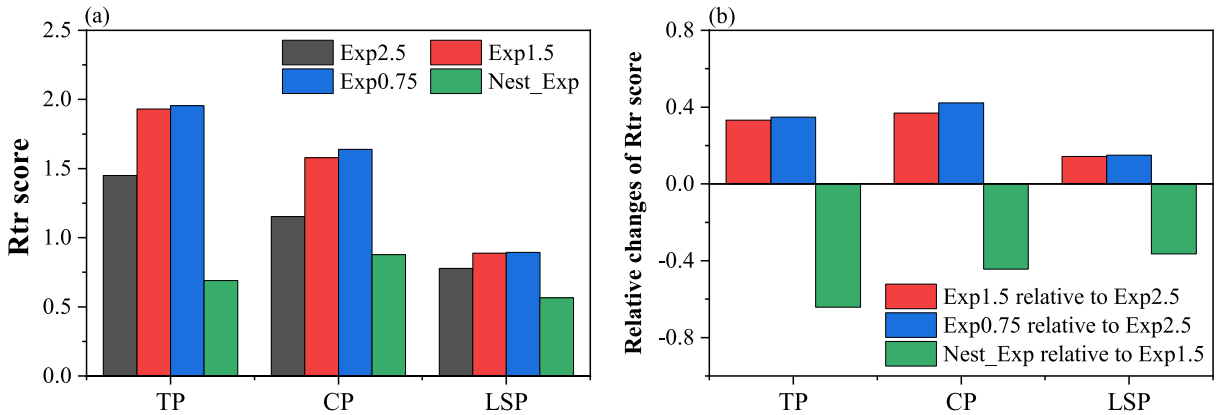

Figure 6. Rtr score of each experiment in simulating the total (TP), convective (CP), and large-scale precipitation (LSP) over the region bounded by 110–120°N and 27–35°E during 1989–1999 (a) and relative changes of Rtr score produced by Exp1.5 and Exp0.75 relative to Exp2.5 and the Nest_Exp relative to Exp1.5 (b).

activity (Xie et al., 2006; Zhou et al., 2018). Compared to Exp2.5, Exp1.5, and Exp0.75, the LBC from finer reanalysis data can improve the skill of CP simulation with the PCC between simulation and ERA5 data increased by 0.08 and 0.02, respectively. However, the Nest_Exp produced a PCC of −0.1, implying that the double-nested downscaling method cannot reproduce the spatial distribution of observed CP.

From Figures 5i–AUTHOR: Please check whether the changes made to the sentence " It may be …" are correct.5l, all experiments overestimated (underestimated) the LSP over most regions north (south) to Yangtze River. Overall, from the simulations of direct downscaling experiments (Figures 5i–5k), adopting the reanalysis data with a finer horizontal resolution to generate the LBC tends to obtain better LSP simulation in terms of PCC. In contrast to the direct downscaling experiments, the Nest_Exp cannot produce a spatial pattern of the observed LSP with a PCC of −0.3. Generally, the RegCM4.6 model with a horizontal resolution of 20 km shows much better performance in simulating CP than LSP. The reason being it may be benefited from the refined description of the detailed information, such as terrain height and land cover types of the land surface (Beck et al., 2004; Bozkurt et al., 2019). In addition, the LSP is mainly controlled by large-scale circulation backgrounds such as monsoon, Meiyu front, etc. (Espinoza et al., 2015; Zhang et al., 2008). Compared to the results of Nest_Exp, the direct downscaling experiments show much better performance in simulating the spatial pattern of precipitation, this may be attributed to the large-scale circulation background from the LBC directly derived from the reanalysis data being better than that produced by the double-nested downscaling method. A more detailed analysis will be shown in the following sections.

Figure 6 displays the Rtr score for the TP, CP, and LSP in summer simulated by each experiment. Compared to Exp2.5, Exp1.5 and Exp0.75 produced a much higher Rtr score (Figures 6a and 6b). Meanwhile, the Rtr score produced by Exp1.5 and Exp0.75 is comparable. It is noted that the skill can be improved by using the LBC derived from the reanalysis data with much higher resolution to a certain degree. However, the improvement is limited when the resolution of reanalysis data for LBC generation reaches a certain threshold (i.e., Exp1.5 and Exp0.75).

To further reveal what leads to the biases in the modeled summer precipitation and 2 m air temperature, we first analyze the differences of several modeled basic meteorological elements from ERA5 data over the internal and lateral boundary areas of the model domain. Figure 7 gives the profile of differences in each element between the simulation from each experiment and ERA5 data regionally averaged over the internal and lateral boundary areas in summer during 1989–1999. The profiles of differences in all elements over the internal area show consistent distribution to those over the lateral boundary area. In another word, the biases can propagate from the lateral boundary area to the internal area of the model domain. The model biases over the internal area mainly result from the LBC, whose quality is one of the key factors affecting the model performance (Giorgi & Mearns, 1999). The similar structure of errors in the LBC for the 3 direct downscaling experiments (Figure 7) led to slight differences in the simulated 2 m air temperature and precipitation (Figures 2–4). However, the Nest_Exp with much larger errors in the LBC resulted in larger biases (Figure 7) in the model 2 m air temperature and precipitation relative to the direct downscaling experiments (Figures 2–4).

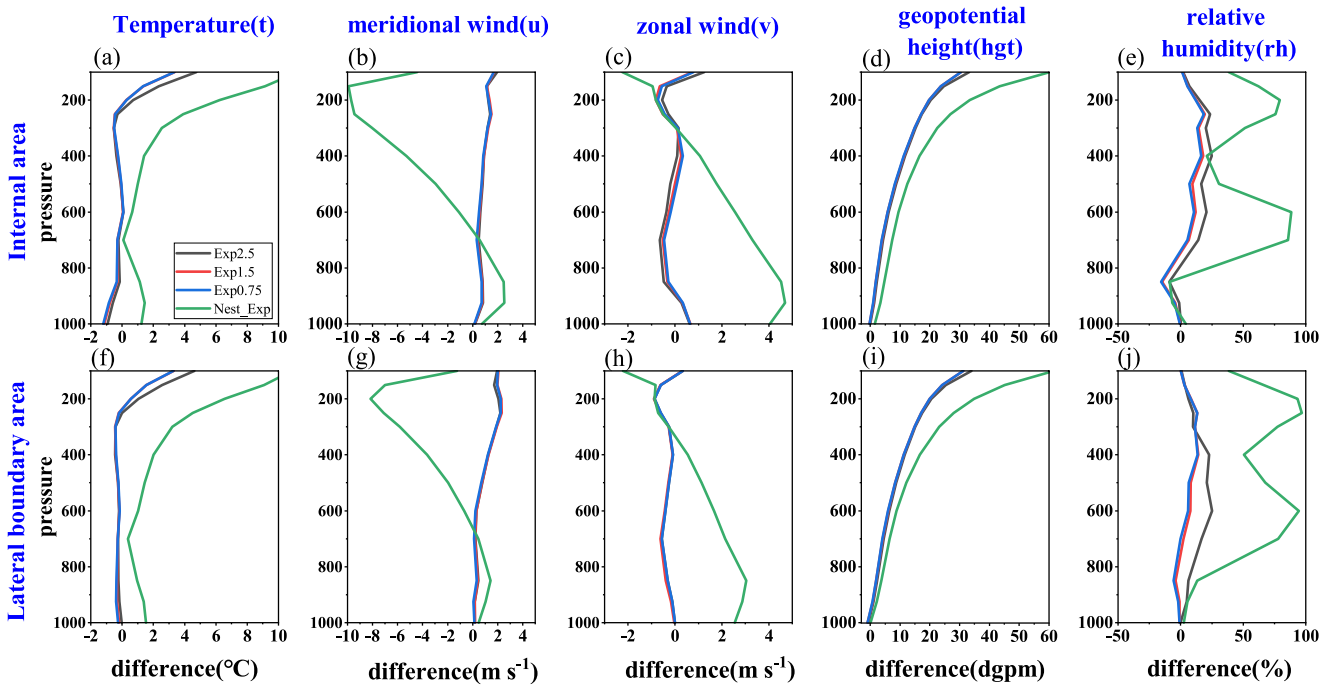

Figure 7. The profiles of differences in each modeled atmospheric variable relative to ERA5 data averaged over the inner area (107–122°E and 27–35°N) and lateral boundary areas (104.5–125°E and 34.5–37°N; 104.5–125°E and 24.5–27°N; 104.5–107°E and 24.5–37°N; and 123–125.5°E and 24.5–37°N) in summer during 1989–1999.

Figure 8 further shows the differences in geopotential height and wind field at 500 and 850 hPa levels in summer averaged during 1989–1999. From Figure 8, the positive deviation of geopotential height propagated from the lateral boundary (Figures 7d and 7i) is much more intuitive over the model domain. All experiments produced stronger geopotential height relative to ERA5 data at 500 and 850 hPa levels. The direct downscaling experiments produced an anomalous vortex at the lower and middle troposphere located in Jianghuai Valley (Figures 8a–8c and 8e–8g), which contributed to the wet biases in LSP (Figure 5). Although Nest_Exp produced an anomalous vortex in the southwest part of the model domain and stronger southwest wind over the most area (Figures 8d and 8h), which lead to the overestimated precipitation in parts of the north Yangtze River

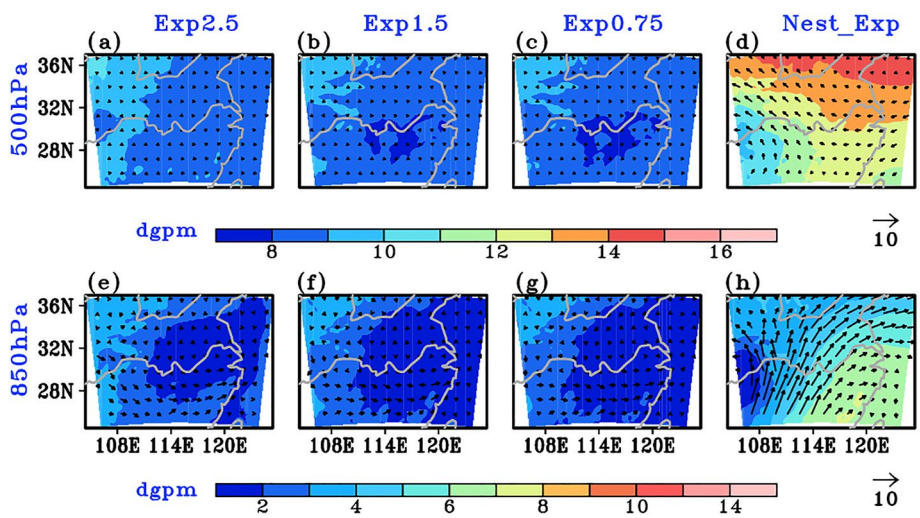

Figure 8. The difference of modeled geopotential height (shaded) and wind field (vector) against ERA5 data at 500 and 850 hPa levels in summer averaged during 1989–1999.

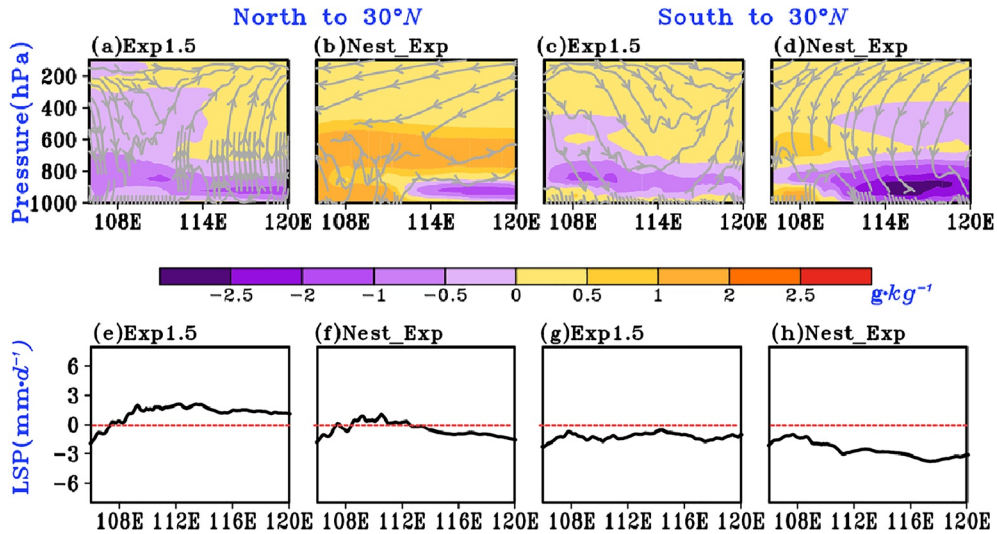

Figure 9. The difference of atmospheric circulation profile (stream), specific humidity (shaded), and large-scale precipitation (line) against ERA5 data regionally averaged over the areas north (a, b, e, and f) and south to 30°N (c, d, g, and h) in summer during 1989–1999.

(Figure 3), the underestimated LSP over the most southeast part of the domain (Figure 5) can be mainly attributed to much-overestimated geopotential height (Figure 8h).

According to Figures 5i–5l, the distribution of LSP in the simulated region is wet (dry) over the region north (south) to 30°N. Therefore, to avoid the process of averaging causing positive and negative cancellation, we divided the nested domain into two subareas. To further reveal the relationship between anomalous atmospheric circulation from simulation and bias of LSP, Figure 9 gives the difference of the longitude-height distribution of the atmospheric circulation, specific humidity, and large-scale precipitation against ERA5 data regionally averaged over the areas north to 30°N and south to 30°N in summer during 1989–1999, respectively. In the area north to 30°N (Figures 9a, 9b, 9e, and 9f), the descending motion with the negative bias of specific humidity in Exp1.5 over west of 110°E results in the dry bias of LSP over this region. Meanwhile, the ascending motion in most levels with the positive bias of specific humidity over 700 hPa levels account for the wet bias over the area along 110°E–120°E (Figures 9 and 9e). In addition, the anomalous updraft in the lower troposphere along 106°E–110°E leads to the wet bias of LSP in the Nest_Exp over this area. However, the negative bias of specific humidity and anomalous downdraft restrain the generation of precipitation and thereafter dry bias in the area along 112°E–120°E (Figures 9b and 9f).

In the area south to 30°N (Figures 9c, 9d, 9g, and 9h), all experiments produce dry bias in LSP (Figures 5i–5l). The Exp1.5 tends to show anomalous descending motion in most layers with the negative bias of specific humidity in the lower troposphere, corresponding to the dry bias of LSP over this region (Figures 9c and 9g). Furthermore, the strong dry downdraft over the whole troposphere in Nest_Exp accounts for the dry bias of LSP with the maximal bias of 4.3 $mm{\cdot}d^{-1}$ (Figures 9d and 9h). In general, the direct downscaling experiments produce wet bias in LSP over the region north to Yangtze River and dry bias over the area south to Yangtze River. And the Nest_Exp shows dry bias over most parts of the model domain, which well corresponds to the bias in the atmospheric circulation.

The convective precipitation mainly results from the abundant water vapor transport and strong uplift (Bozkurt et al., 2019). To reveal what leads to the errors of modeled CP in the two group experiments, Figure 10 shows the differences in water vapor convergence flux (WVCF) between simulation and ERA5 data. The WVCF can be calculated according to Equation 5. From Figures 10a–10c, all of the direct downscaling experiments tend to produce positive biases of WVCF over the northwest of the model domain and the areas south to Yangtze River, indicating much stronger water vapor convergence and ascending motion over these regions with complex terrain leading to the wet biases of CP simulation (Figures 5e–5g). However, among the direct downscaling experiments, the WVCF biases are comparable, suggesting that the influence of LBC derived from the reanalysis data with

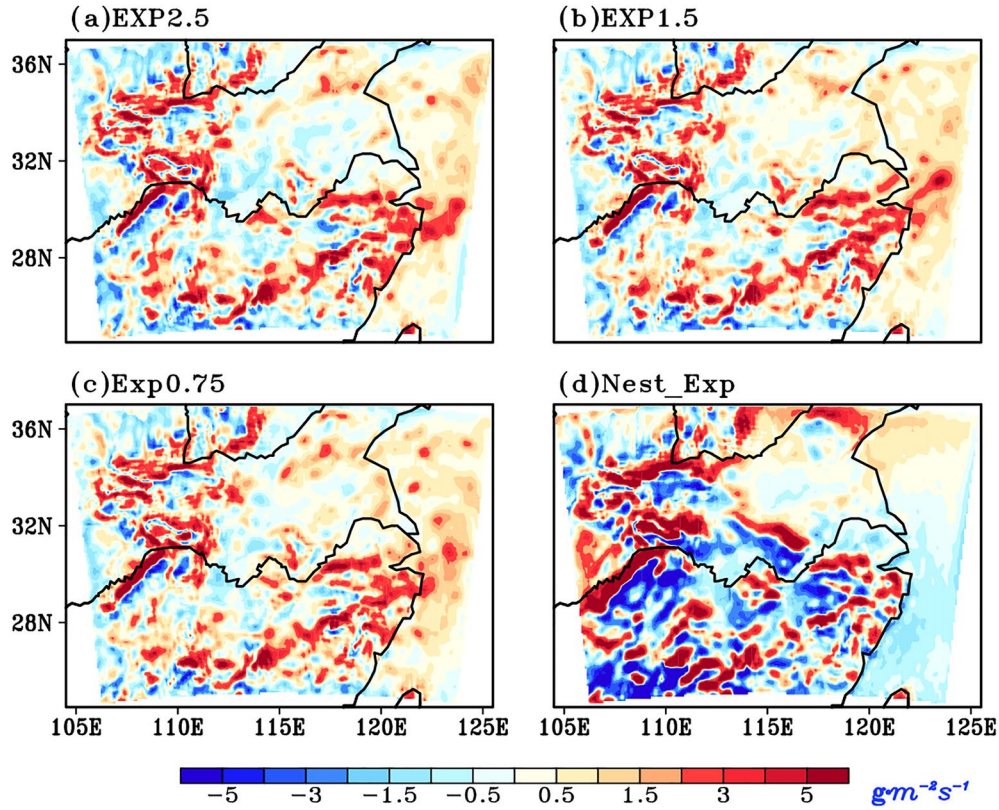

Figure 10. The differences in the modeled water vapor convergence flux against ERA5 data in summer averaged during 1989–1999.

different resolutions on CP is slight. In addition, the negative biases of WVCF produced by the Nest_Exp over most areas south to the Yangtze River (Figure 10d) lead to the underestimation of CP (Figure 5h) over those regions, despite abundant water vapor in the discrete area (Figure 8h).

Figure 11 gives the schematic diagram to illustrate the mechanism related to the bias of precipitation simulation. From the direct downscaling experiments, the modeled anomalous vortex against ERA5 data located in Jiang-Huai Valley accounts for the wet updraft resulting in the wet bias of LSP (Figures 5, 8, and 9). In addition, the discrete positive bias of WVCF mainly leads to the wet bias of CP over the west and parts of the south model domain with complex terrain (Figures 5 and 10). For the double-nested experiment, due to the propagation and accumulation of the errors in the lateral boundary (particularly wind and geopotential height) (Figure 7), the

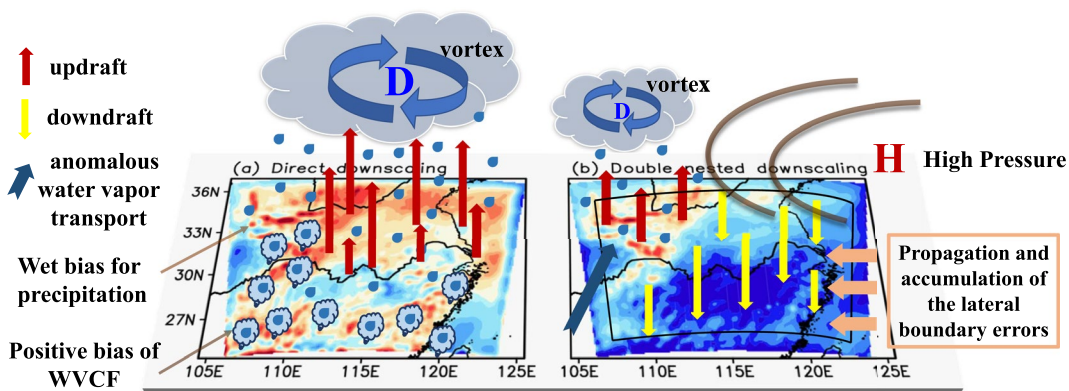

Figure 11. The diagram of the mechanism related to the bias of modeled precipitation over central eastern China in summer.

atmospheric circulation biases featured by high pressure with stronger dry downdraft (Figure 8) lead to the dry bias of LSP over most parts of the model domain, despite a wet bias of precipitation over the northwest influenced by the anomalous vortex (Figure 9). In general, compared to the direct downscaling experiments, the double-nested experiment shows much lower skill in simulating the 2 m air temperature and precipitation over central eastern China in summer (Figure 4).

4. Concluding Remarks and Discussions

In this study, we have investigated the impact of the horizontal resolution of LBC and downscaling approach on the performance of RegCM4.6 with a 20-km horizontal resolution in simulating the 2 m air temperature and precipitation over central eastern China and indicated the possible causes related to the differences in model performance. The main conclusions are summarized as follows:

The direct downscaling experiments consistently outperform the double-nested experiment to simulate the 2 m air temperature and precipitation over central eastern China, suggesting that adopting the direct downscaling method is appropriate to simulate the surface climate over central eastern China. Meanwhile, the direct downscaling experiments driven by the LBC derived from the reanalysis data with the horizontal resolution ranging from 0.75° to 2.5° display very comparable performance with a little better performance by adopting the LBC derived from the reanalysis data of much finer resolution.

Further mechanism analysis indicates that much larger errors of LBC produced by the double-nested downscaling method lead to the positive pressure biases and negative biases of water vapor convergence flux over Jianghuai Valley, which contribute to the much larger biases of precipitation and 2 m air temperature in the double-nested downscaling experiment compared to the direct downscaling experiments. For the direct downscaling experiments, the main causes for wet bias of total precipitation are the anomalous vortex at 850 hPa levels over Jianghuai Valley and the positive bias of water vapor convergence flux in most parts of Yangtze River with complex terrain.

From the result of this study, the main cause of the dissatisfied performance of Nest_Exp has resulted from the accumulation and propagation of bias of LBC. However, as mentioned, the double-nested downscaling method is region-dependent (Hong et al., 2010; Im et al., 2006) and case-dependent (Gu et al., 2020; Raffa et al., 2021), which needs more checkout when using different models in different regions. In addition, all experiments still existed with the overestimated precipitation in the north of the model domain. As we know, many factors can significantly affect the precipitation simulation, especially the configuration of model parameterization (Gao et al., 2016; Gao & Giorgi, 2017a; Hu et al., 2016; Yang et al., 2018; Zhang et al., 2015). In this study, we used the default configuration of the RegCM4 to analyze the initial performance under the different resolutions of LBC and the nested strategy. In the future, studies on the sensitivity of model performance using the double-nested downscaling method to different physical parameterizations should be further addressed in central eastern China.

Data Availability Statement

Data—the reanalysis data with different resolutions from the European Centre for Medium-Range Weather Forecasts (ECMWF) (available at http://apps.ecmwf.int/datasets/data/Interim-full-daily/levtype=sfc/), the sea surface temperature data are the National Oceanic and Atmospheric Administration (NOAA) Optimum Interpolation (OI) SST V2 data (available at https://www.psl.noaa.gov/data/gridded/data.noaa.oisst.v2.html), the fifth generation of ECWMF atmospheric reanalysis data (ERA5) (available at https://cds.climate.copernicus.eu/cdsapp#!/search?type=dataset), and the daily observed precipitation data set SURF_CLI_CHN_PRE_MON_GRID_0.5_V2.0 (available at http://data.cma.cn/) are used in this study. Software—Figures 1–3, 5, 6, and 8–10 were made with the Grid Analysis and Display System (GrADS) V2.2.0 (COLA, 2017, available under the terms of the GNU (2015) General Public License at ftp://cola.gmu.edu/grads/2.2/grads-2.2.0-src.tar.gz). Figures 4 and 7 were made with OriginPro (OriginLab) and can be purchased at https://store.originlab.com/store/Default.aspx?CategoryID=0 and free tried at https://www.originlab.com/try. Figures 1, 9, and 11 were made with Adobe Illustrator CC 2018 (Adobe, 2018) and can be purchased and free tried at https://www.adobe.com/products/illustrator.html.

Acknowledgments
We appreciate the National Natural Science Foundation of China under Grant 41975081, CAS "Light of West China" Program (E12903010 and Y929641001), the Research Funds for the Frontiers Science Center for Critical Earth Material Cycling Nanjing University, the Fundamental Research Funds for the Central Universities (020914380103), the Jiangsu University "Blue Project" outstanding young teachers training object, and the Jiangsu Collaborative Innovation Center for Climate Change. We appreciate the two anonymous reviewers for their insightful and constructive suggestions to help us significantly improve the manuscript.

References

Adeniyi, M. O. (2020). Sensitivity of two dynamical cores in RegCM4. 7 to the 2012 intense rainfall events over West Africa with focus on Lau, Nigeria. *International Journal of Modelling and Simulation*, *40*(5), 355–365. https://doi.org/10.1080/02286203.2019.1641777

Adobe. (2018). Adobe illustrator CC 2018 [software]. Adobe. Retrieved from https://www.adobe.com/products/illustrator.html

Amengual, A., Romero, R., Homar, V., Ramis, C., & Alonso, S. (2007). Impact of the lateral boundary conditions resolution on dynamical downscaling of precipitation in Mediterranean Spain. *Climate Dynamics*, *29*(5), 487–499. https://doi.org/10.1007/s00382-007-0242-0

Beck, A., Ahrens, B., & Stadlbacher, K. (2004). Impact of nesting strategies in dynamical downscaling of reanalysis data. *Geophysical Research Letters*, *31*(19), L19101. https://doi.org/10.1029/2004GL020115

Bozkurt, D., Rojas, M., Boisier, J. P., Rondanelli, R., Garreaud, R., & Gallardo, L. (2019). Dynamical downscaling over the complex terrain of southwest South America: Present climate conditions and added-value analysis. *Climate Dynamics*, *53*(11), 6745–6767. https://doi.org/10.1007/s00382-019-04959-y

Bretherton, C. S., McCaa, J. R., & Grenier, H. (2004). A new parameterization for shallow cumulus convection and its application E1198 KALMÁR ET AL.to marine subtropical cloud-topped boundary layers. Part I: Description and 1D results. *Monthly Weather Review*, *132*(4), 864–882. https://doi.org/10.1175/1520-0493(2004)132<0864:ANPFSC>2.0.CO;2

Bromwich, D. H., Otieno, F. O., Hines, K. M., Manning, K. W., & Shilo, E. (2013). Comprehensive evaluation of polar weather research and forecasting model performance in the Antarctic. *Journal of Geophysical Research: Atmospheres*, *118*(2), 274–292. https://doi.org/10.1029/2012JD018139

Chen, L., Huang, G., & Wang, X. (2019). Projected changes in temperature, precipitation, and their extremes over China through the RegCM. *Climate Dynamics*, *53*(9), 5859–5880. https://doi.org/10.1007/s00382-019-04899-7

Chu, Q., Xu, Z., Chen, Y., & Han, D. (2017). Evaluation of the WRF model with different domain configurations and spin-up time in reproducing a sub-daily extreme rainfall event in Beijing, China. *Hydrology and Earth System*. https://doi.org/10.5194/hess-2017-363

COLA. (2017). The grid analysis and Display system (GrADS) [software]. oceanland-atmosphereCOLA. George Mason University. Retrieved from ftp://cola.gmu.edu/grads/2.2/grads-2.2.0-src.tar.gz

Combes, V., & Matano, R. P. (2014). A two-way nested simulation of the oceanic circulation in the Southwestern Atlantic. *Journal of Geophysical Research: Oceans*, *119*(2), 731–756. https://doi.org/10.1002/2013JC009498

Copernicus Climate Change Service (C3S). (2017). ERA5: Fifth generation of ECMWF atmospheric reanalysis of the global climate. Copernicus Climate Change Service Climate Data Store (CDS), date of access. Retrieved from https://cds.climate.copernicus.eu/cdsapp%23%21/home

Cui, X., Langmann, B., & Graf, H. F. (2007). Summer monsoonal rainfall simulation on the Tibetan Plateau with a regional climate model using a one-way double-nesting system. *Sola*, *3*, 49–52. https://doi.org/10.2151/sola.2007-013

Dee, D. P., Uppala, S. M., Simmons, A. J., Berrisford, P., Poli, P., Kobayashi, S., et al. (2011). The ERA-Interim reanalysis: Configuration and performance of the data assimilation system. *Quarterly Journal of the Royal Meteorological Society*, *137*(656), 553–597. Retrieved from https://rmets.onlinelibrary.wiley.com/doi/full/10.1002/qj.828

Denis, B., Côté, J., & Laprise, R. (2002). Spectral decomposition of two-dimensional atmospheric fields on limited-area domains using the discrete cosine transform (DCT). *Monthly Weather Review*, *130*(7), 1812–1829. https://doi.org/10.1175/1520-0493(2002)130<1812:SDOTDA>2.0.CO;2

Denis, B., Laprise, R., & Caya, D. (2003). Sensitivity of a regional climate model to the resolution of the lateral boundary conditions. *Climate Dynamics*, *20*(2–3), 107–126. https://doi.org/10.1007/s00382-002-0264-6

Denis, B., Laprise, R., Caya, D., & Côté, J. (2002). Downscaling ability of one-way nested regional climate models: The big-brother experiment. *Climate Dynamics*, *18*(8), 627–646. https://doi.org/10.1007/s00382-001-0201-0

Diaconescu, E. P., Gachon, P., & Laprise, R. (2015). On the remapping procedure of daily precipitation statistics and indices used in regional climate model evaluation. *Journal of Hydrometeorology*, *16*(6), 2301–2310. https://doi.org/10.1175/jhm-d-15-0025.1

Diallo, I., Giorgi, F., & Stordal, F. (2018). Influence of Lake Malawi on regional climate from a double-nested regional climate model experiment. *Climate Dynamics*, *50*(9), 3397–3411. https://doi.org/10.1007/s00382-017-3811-x

Dickinson, R. E. (1993). Biosphere atmosphere transfer scheme (BATS) version 1e as coupled to the NCAR community climate model. *NCAR Tech. Note TH-387+ STR*. Retrieved from https://ci.nii.ac.jp/naid/10004840034/

Emanuel, K. A., & Živković-Rothman, M. (1999). Development and evaluation of a convection scheme for use in climate models. *Journal of the Atmospheric Sciences*, *56*(11), 1766–1782. https://doi.org/10.1175/1520-0469(1999)056<1766:DAEOAC>2.0.CO;2

Espinoza, J. C., Chavez, S., Ronchail, J., Junquas, C., Takahashi, K., & Lavado, W. (2015). Rainfall hotspots over the southern tropical Andes: Spatial distribution, rainfall intensity, and relations with large-scale atmospheric circulation. *Water Resources Research*, *51*(5), 3459–3475. https://doi.org/10.1002/2014WR016273

Fu, S. M., Tang, H., Li, Y., Ma, H., & Sun, J. H. (2021). On the relationship of a low-level jet and the formation of a heavy-rainfall-producing mesoscale vortex over the Yangtze River basin. *Atmosphere*, *12*(2), 156. https://doi.org/10.3390/atmos12020156

Gao, X. J., & Giorgi, F. (2017a). Use of the RegCM system over East Asia: Review and perspectives. *Engineering*, *3*(5), 766–772. https://doi.org/10.1016/J.ENG.2017.05.019

Gao, X. J., Shi, Y., & Giorgi, F. (2016). Comparison of convective parameterizations in RegCM4 experiments over China with CLM as the land surface model. *Atmospheric and Oceanic Science Letters*, *9*(4), 246–254. Retrieved from https://www.tandfonline.com/doi/pdf/10.1080/16742834.2016.1172938?needAccess=true

Gao, X. J., Shi, Y., Han, Z., Wang, M., Giorgi, F., Zhang, D., et al. (2017b). Performance of RegCM4 over major river basins in China. *Advances in Atmospheric Sciences*, *34*(4), 441–455. https://doi.org/10.1007/s00376-016-6179-7

Gao, X. J., Xu, Y., Zhao, Z., Pal, J. S., & Giorgi, F. (2006). On the role of resolution and topography in the simulation of East Asia precipitation. *Theoretical and Applied Climatology*, *86*(1), 173–185. https://doi.org/10.1007/s00704-005-0214-4

Giorgi, F., Coppola, E., Solmon, F., Bi, X., Elguindi, N., Nair, V., et al. (2012). RegCM4: Model description and preliminary tests over multiple CORDEX domains. *Climate Research*, *52*, 7–29. https://doi.org/10.3354/cr01018

Giorgi, F., Marinucci, M. R., & Bates, G. T. (1993a). Development of a second-generation regional climate model (RegCM2). Part I: Boundary-layer and radiative transfer processes. *Monthly Weather Review*, *121*(10), 2794–2813. https://doi.org/10.1175/1520-0493(1993)121<2794:DOASGR>2.0.CO;2

Giorgi, F., Marinucci, M. R., Bates, G. T., & De Canio, G. (1993b). Development of a second-generation regional climate model (RegCM2). Part II: Convective processes and assimilation of lateral boundary conditions. *Monthly Weather Review*, *121*(10), 2814–2832. https://doi.org/10.1175/1520-0493(1993)121<2814:DOASGR>2.0.CO;2

Giorgi, F., & Mearns, L. O. (1999). Introduction to special section: Regional climate modeling revisited. *Journal of Geophysical Research*, *104*(D6), 6335–6352. https://doi.org/10.1029/98JD02072

GNU. (2015). The GNU Fortran compiler [software]. GNU, Free Software Foundation, Inc. Retrieved from https://gcc.gnu.org/wiki/GFortranSource

Gu, H., Wang, G., Yu, Z., & Mei, R. (2012). Assessing future climate changes and extreme indicators in east and south Asia using the RegCM4 regional climate model. *Climatic Change*, *114*(2), 301–317. https://doi.org/10.1007/s10584-012-0411-y

Gu, H., Yu, Z., Richard, P. W., & Wang, X. (2020). Sensitivity studies and comprehensive evaluation of RegCM4. 6.1 high-resolution climate simulations over the Tibetan Plateau. *Climate Dynamics*, *54*(7–8), 3781–3801. https://doi.org/10.1007/s00382-020-05205-6

Hassan, M., Pengfei, D., Iqbal, W., & Ba, W. (2015). Dynamic downscaling of South Asia summer monsoon precipitation over COREDEX South Asia using the regional climate model (RegCM4. 3). In *EGU General Assembly Conference Abstracts* (p. 4359). Retrieved from https://ui.adsabs.harvard.edu/abs/2015EGUGA..17.4359H/abstract

Heikkilä, U., Sandvik, A., & Sorteberg, A. (2011). Dynamical downscaling of ERA-40 in complex terrain using the WRF regional climate model. *Climate Dynamics*, *37*(7), 1551–1564. https://doi.org/10.1007/s00382-010-0928-6

Hong, S. Y., Moon, N. K., Lim, K. S. S., & Kim, J. W. (2010). Future climate change scenarios over Korea using a multi-nested downscaling system: A pilot study. *Asia-Pacific Journal of Atmospheric Sciences*, *46*(4), 425–435. https://doi.org/10.1007/s13143-010-0024-1

Hsu, P. C., Li, T., Luo, J. J., Murakami, H., Kitoh, A., & Zhao, M. (2012). Increase of global monsoon area and precipitation under global warming: A robust signal? *Geophysical Research Letters*, *39*(6), L06701. https://doi.org/10.1029/2012GL051037

Hu, H., Hu, Y., Zhong, Z., & Zhu, Y. (2015). Double nested dynamical downscaling research on summer precipitation over China with WRF model. *Journal of the Meteorological Sciences*, *35*(4), 413–421. Retrieved from https://en.cnki.com.cn/Article_en/CJFDTotal-QXKX201504005.htm

Hu, Y., Ding, Y., & Liao, F. (2010). An improvement on summer regional climate simulation over East China: Importance of data assimilation of soil moisture. *Chinese Science Bulletin*, *55*(9), 865–871. https://doi.org/10.1007/s11434-009-0285-1

Hu, Y., Zhong, Z., Lu, W., Zhang, Y., & Sun, Y. (2016). Evaluation of RegCM4 in simulating the interannual and interdecadal variations of Meiyu rainfall in China. *Theoretical and Applied Climatology*, *124*(3), 757–767. Retrieved from https://click.endnote.com/viewer?doi=10.1007/s00704-015-1459-1%26route=7

Huang, A., Zhou, Y., Zhang, Y., Huang, D., Zhao, Y., & Wu, H. (2014). Changes of the annual precipitation over central Asia in the twenty-first century projected by multimodels of CMIP5. *Journal of Climate*, *27*(17), 6627–6646. https://doi.org/10.1175/JCLI-D-14-00070.1

Huang, D., & Gao, S. (2018). Impact of different reanalysis data on WRF dynamical downscaling over China. *Atmospheric Research*, *200*, 25–35. https://doi.org/10.1016/j.atmosres.2017.09.017

Im, E. S., Park, E. H., Kwon, W. T., & Giorgi, F. (2006). Present climate simulation over Korea with a regional climate model using a one-way double-nested system. *Theoretical and Applied Climatology*, *86*(1), 187–200. https://doi.org/10.1007/s00704-005-0215-3

Ji, Z., & Kang, S. (2013). Double-nested dynamical downscaling experiments over the Tibetan Plateau and their projection of climate change under two RCP scenarios. *Journal of the Atmospheric Sciences*, *70*(4), 1278–1290. https://doi.org/10.1175/JAS-D-12-0155.1

Kalmar, T., Pieczka, I., Pongracz, R., & Bartholy, J. (2018). Comparison of hydrostatic and non-hydrostatic RegCM regional climate model simulations for the Carpathian region. In *EGU General Assembly Conference Abstracts* (p. 1175).

Kan, M., Huang, A., Zhao, Y., Zhou, Y., Yang, B., & Wu, H. (2015). Evaluation of the summer precipitation over China simulated by BCC_CSM model with different horizontal resolutions during the recent half century. *Journal of Geophysical Research: Atmospheres*, *120*(10), 4657–4670. https://doi.org/10.1002/2015JD023131

Kiehl, J. T., Hack, J. J., Bonan, G. B., Boville, B. A., Briegleb, B. P., Williamson, D. L., & Rasch, P. J. (1996). Description of the NCAR community climate model (CCM3). Technical Note (No. PB-97-131528/XAB; NCAR/TN-420-STR). National Center for Atmospheric Research, Boulder, CO (United States). Climate and Global Dynamics Div https://www.osti.gov/biblio/442361

Kong, X., Wang, A., Bi, X., & Wang, D. (2019). Assessment of temperature extremes in China using RegCM4 and WRF. *Advances in Atmospheric Sciences*, *36*(4), 363–377. https://doi.org/10.1007/s00376-018-8144-0. Retrieved from https://link.springer.com/content/pdf/10.1007/s00376-018-8144-0.pdf

Laprise, R., Kornic, D., Rapaić, M., Šeparović, L., Leduc, M., Nikiema, O., et al. (2012). Considerations of domain size and large-scale driving for nested regional climate models: Impact on internal variability and ability at developing small-scale details. In *Climate change* (pp. 181–199). Springer. Retrieved from https://link.springer.com/chapter/10.1007/978-3-7091-0973-1_14

Leps, N., Brauch, J., & Ahrens, B. (2019). Sensitivity of limited area atmospheric simulations to lateral boundary conditions in idealized experiments. *Journal of Advances in Modeling Earth Systems*, *11*(8), 2694–2707. https://doi.org/10.1029/2019MS001625

Leung, L. R., & Qian, Y. (2003). The sensitivity of precipitation and snowpack simulations to model resolution via nesting in regions of complex terrain. *Journal of Hydrometeorology*, *4*(6), 1025–1043. https://doi.org/10.1175/1525-7541(2003)004<1025:TSOPAS>2.0.CO;2

Lin, H. Y., Hu, J. M., Chen, T. Y., Hsieh, C. F., Wang, G., Wang, T., et al. (2018). A dynamic downscaling approach to generate scale-free regional climate data in Taiwan. *Taiwania*, *63*(3).

Liu, S., Liang, X. Z., Gao, W., He, Y., & Ling, T. (2011). Regional climate model simulations of the 1998 summer China flood: Dependence on initial and lateral boundary conditions. *The Open Atmospheric Science Journal*, *5*(1), 96–105. https://doi.org/10.2174/1874282301105010096

Marbaix, P., Gallée, H., Brasseur, O., & van Ypersele, J. P. (2003). Lateral boundary conditions in regional climate models: A detailed study of the relaxation procedure. *Monthly Weather Review*, *131*(3), 461–479. https://doi.org/10.1175/1520-0493(2003)131<0461:LBCIRC>2.0.CO;2

Maurya, R. K. S., Sinha, P., Mohanty, M. R., & Mohanty, U. C. (2018). RegCM4 model sensitivity to horizontal resolution and domain size in simulating the Indian summer monsoon. *Atmospheric Research*, *210*, 15–33. https://doi.org/10.1016/j.atmosres.2018.04.010

Meng, C., Ma, Y., Ma, W., & Xu, Y. (2018). Modeling of a severe winter drought in eastern China using different initial and lateral boundary forcing datasets. *Theoretical and Applied Climatology*, *133*(3), 763–773. https://doi.org/10.1007/s00704-017-2217-3

Ngo-Duc, T., Tangang, F. T., Santisirisomboon, J., Cruz, F., Trinh-Tuan, L., Nguyen-Xuan, T., et al. (2017). Performance evaluation of RegCM4 in simulating extreme rainfall and temperature indices over the CORDEX-Southeast Asia region. *International Journal of Climatology*, *37*(3), 1634–1647. https://doi.org/10.1002/joc.4803

Nguyen-Xuan, T., Lam, S. L., Giorgi, F., Coppola, E., Giuliani, G., Gao, X., & Im, E. S. (2021). Evaluation of the performance of the non-hydrostatic RegCM4 (RegCM4-NH) over southeastern China. *Climate Dynamics*, *1–19*(5–6), 1419–1437. https://doi.org/10.1007/s00382-021-05969-5

Nogherotto, R. (2015). A numerical framework for multiple phase cloud microphysics in regional and global atmospheric models. Retrieved from http://hdl.handle.net/10077/11140

Nogherotto, R., Tompkins, A. M., Giuliani, G., Coppola, E., & Giorgi, F. (2016). Numerical framework and performance of the new multiple-phase cloud microphysics scheme in RegCM4. 5: Precipitation, cloud microphysics, and cloud radiative effects. *Geoscientific Model Development*, *9*(7), 2533–2547. https://doi.org/10.5194/gmd-9-2533-2016

Pal, J. S., Giorgi, F., Bi, X., Elguindi, N., Solmon, F., Gao, X., et al. (2007). Regional climate modeling for the developing world: The ICTP RegCM3 and RegCNET. *Bulletin of the American Meteorological Society*, *88*(9), 1395–1410. https://doi.org/10.1175/BAMS-88-9-1395

Pal, J. S., Small, E. E., & Eltahir, E. A. (2000). Simulation of regional-scale water and energy budgets: Representation of subgrid cloud and precipitation processes within RegCM. *Journal of Geophysical Research*, *105*(D24), 29579–29594. https://doi.org/10.1029/2000JD900415

Pan, X. D., Zhang, L., & Huang, C. L. (2020). Future climate projection in northwest China with RegCM4. 6. *Earth and Space Science*, *7*(2), e2019EA000819. https://doi.org/10.1029/2019EA000819

Park, J. H., Oh, S. G., & Suh, M. S. (2013). Impacts of boundary conditions on the precipitation simulation of RegCM4 in the CORDEX East Asia domain. *Journal of Geophysical Research: Atmospheres*, *118*(4), 1652–1667. https://doi.org/10.1002/jgrd.50159

Pavlik, D., Pavlik, D., Söhl, D., Pluntke, T., Mykhnovych, A., & Bernhofer, C. (2012). Dynamic downscaling of global climate projections for Eastern Europe with a horizontal resolution of 7 km. *Environmental Earth Sciences*, *65*(5), 1475–1482. https://doi.org/10.1007/s12665-011-1081-1

Qi, J., Chen, C., & Beardsley, R. C. (2018). FVCOM one-way and two-way nesting using ESMF: Development and validation. *Ocean Modelling*, *124*, 94–110. https://doi.org/10.1016/j.ocemod.2018.02.007

Raffa, M., Reder, A., Adinolfi, M., & Mercogliano, P. (2021). A comparison between one-step and two-step nesting strategy in the dynamical downscaling of regional climate model COSMO-CLM at 2.2 km driven by ERA5 reanalysis. *Atmosphere*, *12*(2), 260. https://doi.org/10.3390/atmos12020260

Reynolds, R. W., Rayner, N. A., Smith, T. M., Stokes, D. C., & Wang, W. (2002). An improved in situ and satellite SST analysis for climate. *Journal of Climate*, *15*(13), 1609–1625. https://doi.org/10.1175/1520-0442(2002)015<1609:AIISAS>2.0.CO;2

Seth, A., Rauscher, S. A., Camargo, S. J., Qian, J. H., & Pal, J. S. (2007). RegCM3 regional climatologies for South America using reanalysis and ECHAM global model driving fields. *Climate Dynamics*, *28*(5), 461–480. https://doi.org/10.1007/s00382-006-0191-z

Shi, Y., Wang, G., & Gao, X. (2018). Role of resolution in regional climate change projections over China. *Climate Dynamics*, *51*(5), 2375–2396. https://doi.org/10.1007/s00382-017-4018-x

Taylor, K. E. (2001). Summarizing multiple aspects of model performance in a single diagram. *Journal of Geophysical Research*, *106*(D7), 7183–7192. https://doi.org/10.1029/2000JD900719

Wang, X., Yang, M., & Pang, G. (2015). Influences of two land-surface schemes on RegCM4 precipitation simulations over the Tibetan Plateau. *Advances in Meteorology*, 106891–106912. https://doi.org/10.1155/2015/106891

Wu, J., Gao, X., Giorgi, F., Chen, Z., & Yu, D. (2012). Climate effects of the Three Gorges Reservoir as simulated by a high resolution double nested regional climate model. *Quaternary International*, *282*, 27–36. https://doi.org/10.1016/j.quaint.2012.04.028

Wu, W., Lynch, A. H., & Rivers, A. (2005). Estimating the uncertainty in a regional climate model related to initial and lateral boundary conditions. *Journal of Climate*, *18*(7), 917–933. https://doi.org/10.1175/JCLI-3293.1

Xie, S. P., Xu, H., Saji, N. H., Wang, Y., & Liu, W. T. (2006). Role of narrow mountains in large-scale organization of Asian monsoon convection. *Journal of Climate*, *19*(14), 3420–3429. https://doi.org/10.1175/JCLI3777.1

Xue, Y., Janjic, Z., Dudhia, J., Vasic, R., & De Sales, F. (2014). A review on regional dynamical downscaling in intraseasonal to seasonal simulation/prediction and major factors that affect downscaling ability. *Atmospheric Research*, *147*, 68–85. https://doi.org/10.1016/j.atmosres.2014.05.001

Yang, M., Zuo, R., Wang, L., & Chen, X. (2018). Simulation of land surface climate over China with RegCM4. 5: Verification and analysis. *Advances in Meteorology*, *1–14*, 1–14. Retrieved from https://click.endnote.com/viewer?doi=10.1155/2018/7960908%26route=7

Zeng, X., Zhao, M., & Dickinson, R. E. (1998). Intercomparison of bulk aerodynamic algorithms for the computation of sea surface fluxes using TOGA COARE and TAO data. *Journal of Climate*, *11*(10), 2628–2644. https://doi.org/10.1175/1520-0442(1998)011<2628:IOBAAF>2.0.CO;2

Zhang, Q., Xu, C. Y., Zhang, Z., Chen, Y. D., Liu, C. l., & Lin, H. (2008). Spatial and temporal variability of precipitation maxima during 1960–2005 in the Yangtze River basin and possible association with large-scale circulation. *Journal of Hydrology*, *353*(3–4), 215–227. https://doi.org/10.1016/j.jhydrol.2007.11.023

Zhang, S., Lü, S., Bao, Y., & Ma, D. (2015). Sensitivity of precipitation over China to different cumulus parameterization schemes in RegCM4. *Journal of Meteorological Research*, *29*(1), 119–131. https://doi.org/10.1007/s13351-014-4042-2

Zhang, Y., Cai, C., Chen, B., & Dai, W. (2019). Consistency evaluation of precipitable water vapor derived from ERA5, ERA-Interim, GNSS, and radiosondes over China. *Radio Science*, *54*(7), 561–571. https://doi.org/10.1029/2018rs006789

Zhao, T., Fu, C., Ke, Z., & Guo, W. (2010). Global atmosphere reanalysis datasets: Current status and recent advances. *Advances in Earth Science*, *25*(3), 241–254. Retrieved from http://www.adearth.ac.cn/EN/10.11867/j.issn.1001-8166.2010.03.0241

Zhao, T. B., & Fu, C. B. (2006). Preliminary comparison and analysis of reanalysis data and observation data of ERA-40 and NCEP-2 in China. *Climatic and Environmental Research*, *1*, 14–32. Retrieved from https://www.oalib.com/paper/1700030

Zhao, Y., Zhu, J., Yan, X. U., & Center, N. M. (2014). Establishment and assessment of the grid precipitation datasets in China for recent 50 years. *Journal of the Meteorological Sciences*. Retrieved from http://en.cnki.com.cn/Article_en/CJFDTOTAL-QXKX201404009.htm

Zhong, Z., Hu, Y., Min, J., & Xu, H. (2007). Numerical experiments on the spin-up time for seasonal-scale regional climate modeling. *Acta Meteorologica Sinica*, *4*. Retrieved from https://www.cnki.com.cn/Article/CJFDTEMP-QXXW200704003.htm

Zhou, X., Yang, K., & Wang, Y. (2018). Implementation of a turbulent orographic form drag scheme in WRF and its application to the Tibetan Plateau. *Climate Dynamics*, *50*(7), 2443–2455. https://doi.org/10.1007/s00382-017-3677-y